

A Bifunctional Biosensor for Determination of H₂O₂ and NADH Using Polyaniline, Silicomolybdate, and MWCNT Hybrid Composites

Kuo-Chiang Lin, Xiao-Cheng Jian, Shen-Ming Chen*

Electroanalysis and Bioelectrochemistry Lab, Department of Chemical Engineering and Biotechnology, National Taipei University of Technology, No.1, Section 3, Chung-Hsiao East Road, Taipei 106, Taiwan (ROC).

*E-mail: smchen78@ms15.hinet.net

Received: 23 May 2011 / Accepted: 29 June 2011 / Published: 1 August 2011

A hybrid composite of polyaniline (PANI), silicomolybdate (SiMO), and MWCNT has been successfully immobilized on electrode surface. The hybrid composite (PANI/SiMO/MWCNT) is found stable in various scan rate and different pH condition. It exhibits specific SEM image different from PANI, MWCNT, and PANI/SiMO. Under 20 scan cycles, the average surface concentration (Γ) was estimated to be about 2.68×10^{-10} mol cm⁻². This film modified electrode also shows good electrocatalytic properties for NADH and H₂O₂ as compared with other film modified electrodes including PANI/GCE, PANI/SiMO/GCE, and PANI/MWCNT/GCE. Considering the pH condition, it is found that the better electrocatalytic current appears at pH 4 and pH 6 for NADH and H₂O₂, respectively. Further determining these species by amperometry, it shows a linear concentration range of 0.01 – 0.18 mM with a sensitivity of 222.3 μ A mM⁻¹ cm⁻² and a detection limit of 5 μ M (S/N = 3) for NADH ($E_{app.} = +0.35$ V). Applied potential at -0.35 V, it also shows a linear concentration range of 0.0294 – 2.205 mM with a sensitivity of 18.75 μ A mM⁻¹ cm⁻² and a detection limit of 9.2 μ M (S/N = 3) for H₂O₂ determination.

Keywords: Biosensor, hydrogen peroxide, NADH, polyaniline, silicomolybdate, MWCNT

1. INTRODUCTION

The detection of hydrogen peroxide (H₂O₂) plays a significant role in many fields including clinic, food, pharmaceutical and environmental analyses [1]. Thus, several analytical methods have been developed for the detection of H₂O₂, such as fluorescence, chemiluminescence, and electrochemical methods [2–5]. Among these methods, electrochemical detection of H₂O₂ is distinctive for its low detection limit as well as low costs [6,7]. However, most sensors based on enzymes or

proteins may result in limited lifetime, stability problem and complex procedures in the fabrication process. Thus, the development of enzyme-free H_2O_2 sensors with low detection limit and wide responding range has become a trend.

The electrochemical oxidation of nicotinamide adenine dinucleotide (NADH) has received considerable interest due to its very important role as a cofactor in a whole diversity of dehydrogenase-based bioelectrochemical devices such as biosensors, biofuel cells, and bioreactors [8–10]. However, direct oxidation of NADH at a conventional solid electrode is highly irreversible, requires large activation energy, and proceeds with coupled side reactions, poisoning the electrode surface [11–13]. In recent years, many nanomaterials, especially various carbon nanomaterials [14–16], have been used widely to reduce the over-potential for NADH oxidation and minimize the surface contamination effect without the help of redox mediators. However, the analytical performance of the electrochemical NADH sensors based on the carbon nanomaterials often showed narrower linear range [14] or lower sensitivity [16], which needs to be improved to satisfy the need of rapid development of the dehydrogenase-based bioelectrochemical devices.

Among the conducting polymers, polyaniline (PANI) has attracted attention of most of the researchers, due to the combination of unique properties like simple preparation and doping procedure, good environmental stability, relatively high conductivity and low cost and also due to their wide spectrum of applications [17, 18]. Due to its chemical, electrical, and optical properties, PANI has been widely studied and used in rechargeable batteries [19, 20] and electrocatalysis [21–27].

Silicomolybdate (SiMO) polyoxometalate, $\text{SiMo}_{12}\text{O}_{40}^{4-}$, form nanometer-sized polyoxometalate clusters that are of interest in bioanalysis, material science, catalysis, magnetism, surface chemistry and medicine. The polyoxometalate anion is a mixed-valence species and polyoxometalate modified electrodes and their electrocatalytic properties are very important and are the subject of intensive research. Some polyoxometalate modified electrodes have been reported in the literature concerning nanostructured organic and inorganic hybrid films [28–36].

Carbon nanotubes have emerged as promising nanomaterials for the fabrication of electronic devices and sensors due to their extraordinary physical and electrical properties such as high tensile strength, high elastic modules, high thermal conductivity and electrical conductivity [37, 38]. The carbon nanotubes usually have high surface area to weight ratio of $300 \text{ m}^2 \text{ g}^{-1}$, and most of this surface area is accessible to both electrochemistry and immobilization of the biomolecules [39]. Unique electrical properties together with significant surface enlargement make them an important component in sensing applications. MWCNTs have been extensively used in the fabrication of electrochemical biosensors due to their excellent electrocatalytic activity and antifouling properties [40–43]. Their use in these devices is based on the fact that MWCNTs can play dual roles. They can be easily used as immobilization platform for biomolecules, while at the same time they can relay the electrochemical signal acting as transducers. As electrode materials, MWCNTs can be used for promoting electron transfer between the electroactive species and the electron and provide a novel platform for designing electrochemical biosensors.

In this work, we plan to fabricate an enzyme-free and bifunctional biosensor using PANI, SiMO, and MWCNT. Here, we report a simple method to immobilize PANI, SiMO, and MWCNT on electrode surface for electrocatalysis study of NADH and H_2O_2 . The hybrid film was characterized by

cyclic voltammetry and scanning electron microscopy. The electrocatalytic property was also studied and compared with other different modified electrodes including PANI, PANI/SiMO, and PANI/MWCNT modified electrodes. The quantitative determination of NADH and H₂O₂ was further investigated by amperometry.

2. EXPERIMENTAL

2.1. Reagents

Aniline monomer, silicomolybdate (SiMO), multi-wall carbon nanotube (MWCNT), hydrogen peroxide (H₂O₂), and nicotinamide adenine dinucleotide (NADH), were purchased from Sigma-Aldrich (USA). All other chemicals (Merck) used were of analytical grade (99%). Double distilled deionized water (DDDW) was used to prepare all the solutions. Such as a pH 1.5 (0.1 M H₂SO₄) was prepared using sulfuric acid to dilute with DDDW. A pH 4 buffer solution was prepared using potassium hydrogen phthalate (0.1 M KHP). A phosphate buffer solution (PBS) of pH 7 was prepared using Na₂HPO₄ (0.05 M) and NaH₂PO₄ (0.05 M). Other higher pH buffer solutions were appropriately adjusted with di-sodium tetraborate, sodium carbonate, and sodium hydroxide, respectively.

2.2. Apparatus

All electrochemical experiments were performed using CHI 1205a potentiostats (CH Instruments, USA). The BAS glassy carbon electrode (GCE) with a diameter of 0.3 cm and exposed geometric surface area of 0.07 cm² (purchased from Bioanalytical Systems, Inc., USA) was used. A conventional three-electrode system was used which consists of an Ag/AgCl (3M KCl) as a reference electrode, a GCE as a working electrode, and a platinum wire as a counter electrode. For the rest of the electrochemical studies, an Ag/AgCl (3M KCl) was used as a reference. Prior to the experiments, the glassy carbon electrode was ultrasonicated in DDDW for 1 min after finishing the polish by Buehler felt pads and alumina power (0.05 μm).

The morphological characterization of composite films was examined by means of SEM (S-3000H, Hitachi). Indium tin oxide (ITO) glass was the substrate coated with different films for SEM analysis. The buffer solution was entirely altered by deaerating with nitrogen gas atmosphere. The electrochemical cells were properly sealed to avoid the oxygen interference from the atmosphere.

2.3. Electrochemical preparation of PANI/SiMO/MWCNT hybrid film

The electrochemical formation of the PANI/SiMO hybrid films was performed by repetitive cycling of the potential of the working electrode in a definite potential between -0.2 V and 0.85 V in a pH 1.5 aqueous solution containing 4×10⁻³ M aniline monomer and 1×10⁻⁴ M silicomolybdate (SiMO). This PANI/SiMO electrode was further adsorbed with 4 μl MWCNT and dried out in room

temperature. After this procedure, the PANI/SiMO/MWCNT was prepared and stored in room temperature to be used.

3. RESULTS AND DISCUSSION

3.1. Cyclic voltammograms of PANI/SiMO/MWCNT modified electrode with various scan rates and pH conditions

In the present work, the PANI and SiMO hybrid film (PANI/SiMO) was firstly modified onto the electrode surface by electro-codeposition.

Then, the MWCNT was further adsorbed on this electrode to form the PANI/SiMO/MWCNT hybrid composite. The electrochemical properties of PANI/SiMO modified GCE were studied with various scan rates and pH solutions by cyclic voltammetry. Fig. 1 shows the cyclic voltammograms of the resulting electrode obtained with various scan rates in 0.1 M H₂SO₄ solution (pH 1.5). The electrochemical response of PANI/SiMO/MWCNT/GCE exhibits four stable redox couples, in which can be attributed to the electron transformations between PANI and SiMO in the hybrid film. Four redox couples were found with formal potential ($E^{0'}$) of $E_1^{0'} = 0.25$ V, $E_2^{0'} = 0.05$ V, $E_3^{0'} = -0.18$ V, and $E_4^{0'} = -0.35$ V. Compared with the previous study, the redox couple 1 is known for polyaniline redox process and the redox couple 2-4 are known for SiMO redox process, viz. ([H₄SiMo₁₂O₄₀]/[H₆SiMo₁₂O₄₀], [H₆SiMo₁₂O₄₀]/[H₈SiMo₁₂O₄₀], [H₈SiMo₁₂O₄₀]/[H₁₀SiMo₁₂O₄₀]) of the SiMo₁₂O₄₀⁴⁻ redox process [44], in the cyclic voltammograms. It is noticed that the film shows not obvious PANI redox peak as compared PANI/SiMO. This might be due to the overlapping with the MWCNT voltammetric background.

The influence of redox peak the PANI/SiMO/MWCNT/GCE on the scan rates was investigated. In the range of 10 – 100 mV s⁻¹, the anodic and cathodic peak currents were both proportional to the scan rate (peak 1 is used to study), implying that the electrochemical kinetics is a surface-controlled process. As can be known from the CVs (inset of Fig. 1A), the redox behavior of PANI/SiMO/MWCNT/GCE, introducing peak current (I_p) was greatly enhanced with the increase of scan rate. Based on Laviron's equation [45] as following equation:

$$I_p = n^2 F^2 \nu A \Gamma / 4RT \quad (1)$$

where A (= 0.0707 cm²) is the area of the glassy carbon electrode, n (= 2) is the number of electrons per reactant molecule, F is the Faraday constant, ν is the scan rate, R is the gas constant, and T is the temperature. We assume that all of the immobilized redox centers are electroactive on the voltammetry time scale and a flat surface. From the slope of the I_p - ν curve for a surface process, the surface concentration (Γ) of PANI was estimated. Under 20 scan cycles, the average surface concentration (Γ) of PANI was estimated to be about 2.68×10^{-10} mol cm⁻².

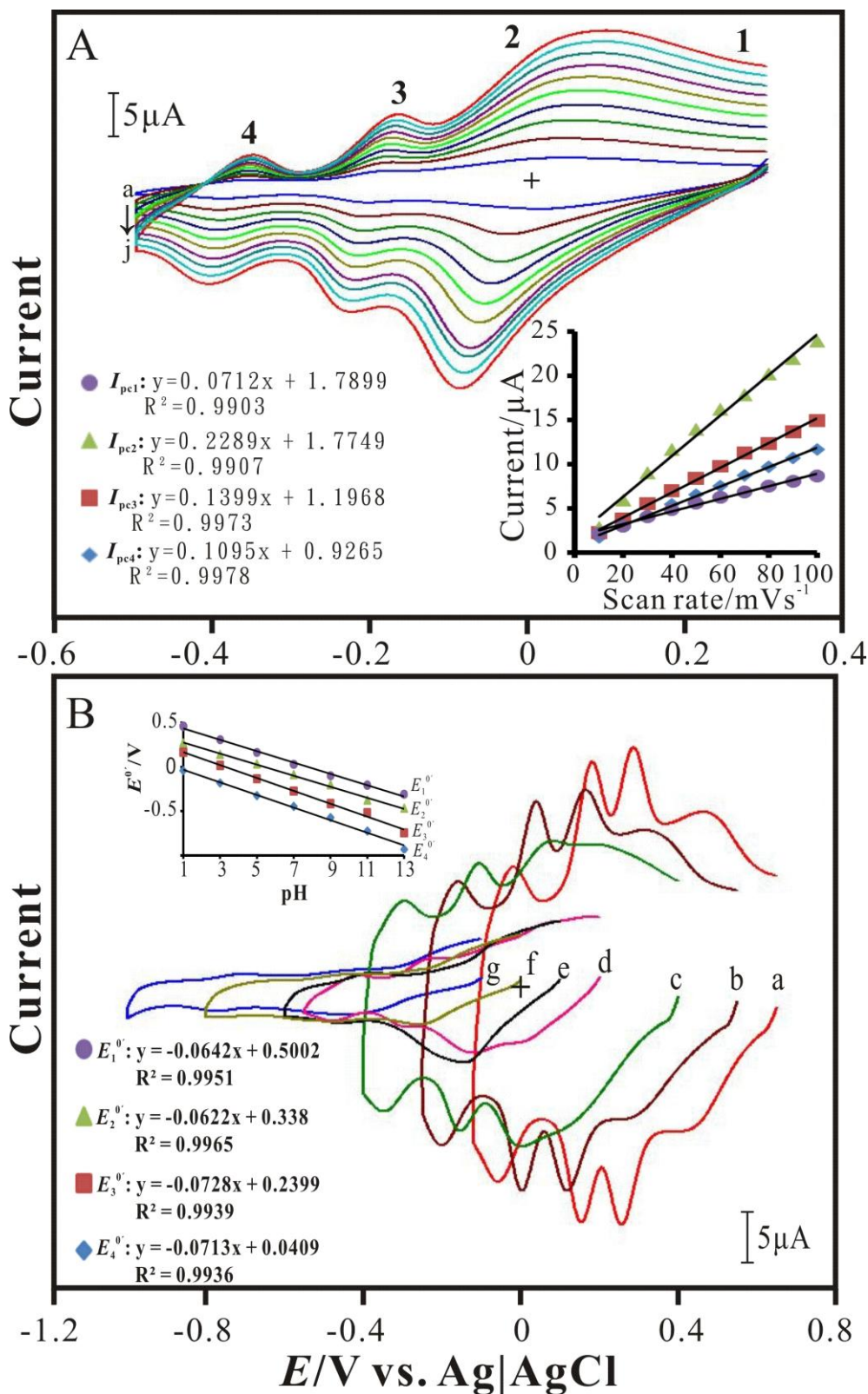


Figure 1. (A) Cyclic voltammograms of PANI/SiMO/MWCNT/GCE examined in 0.1 M H₂SO₄ (pH 1.5) with various scan rate of (a) 10, (b) 20, (c) 30, (d) 40, (e) 50, (f) 60, (g) 70, (h) 80, (i) 90, and (j) 100 mV s⁻¹, respectively. Inset: the plot of cathodic peak current (I_{pc}) vs. scan rate. (B) Cyclic voltammograms of PANI/SiMO/MWCNT/GCE examined at (a) pH 1, (b) pH 3, (c) pH 5, (d) pH 7, (e) pH 9, (f) pH 11, and (g) pH 13, respectively. Scan rate = 0.1 V s⁻¹. Inset: the plot of formal potential ($E^{0'}$) vs. pH.

Fig. 1B displays the pH-dependent voltammetric response of PANI/SiMO/MWCNT modified electrode. In order to ascertain this, the voltammetric responses of PANI/SiMO/MWCNT electrode were obtained in the solutions of different pH values varying from 1 to 13.

The formal potential of these redox couples are pH-dependent with negative shifting as increasing pH value of the buffer solution. The inset of Fig. 1B shows the formal potential ($E_1^{0'}$, $E_2^{0'}$, $E_3^{0'}$, and $E_4^{0'}$) of PANI/SiMO/MWCNT plotted over a pH range of 1–13. $E_1^{0'}$, $E_2^{0'}$, $E_3^{0'}$, and $E_4^{0'}$ represent the formal potential from the positive side to the negative side. The response of PANI redox couple ($E_1^{0'}$) shows a slope of -64.2 mV/pH, which is close to that given by the Nernstian equation for equal number of electrons and protons transfer processes. The SiMO redox couples ($E_2^{0'}$, $E_3^{0'}$, $E_4^{0'}$) shows a slope of -62.2 , -72.8 , and -71.3 mV pH^{-1} , respectively. They are close to that expected from calculations using Nernstian equation. The phenomenon indicates that the number of electrons and protons is the same. In our case, two electrons and two protons were involved in the PANI redox couple, whereas two electrons and two protons were involved in each SiMO redox couple. The above result shows that the PANI/SiMO/MWCNT hybrid film is stable and electrochemically active in the aqueous buffer solutions.

3.2. Morphology of PANI/SiMO/MWCNT hybrid film

Scanning electron microscopy (SEM) was utilized to study the morphology of the active surface of the PANI/SiMO/MWCNT hybrid film.

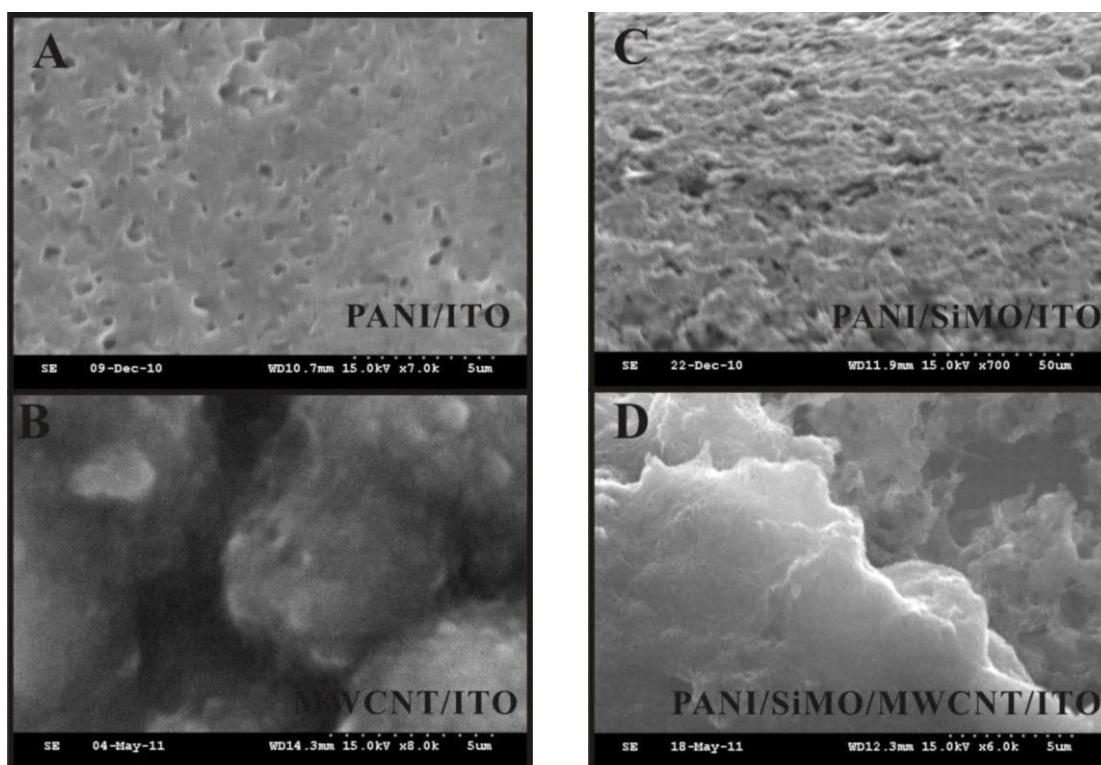


Figure 2. SEM images of (A) PANI/ITO, (B) MWCNT/ITO, (C) PANI/SiMO/ITO, and (D) PANI/SiMO/MWCNT/ITO, respectively.

Fig. 2 shows the single composite SEM images for PANI (Fig. 2A) and MWCNT (Fig. 2B), respectively. Both of them exhibits cluster structure might be due to the formation of PANI polymer chains while the aggregation of MWCNT molecules. Particularly, the hybrid composites of PANI/SiMO (Fig. 2C) and PANI/SiMO/MWCNT (Fig. 2D) shows unique rough surface different from PANI (Fig. 2A) and MWCNT (Fig. 2B). This might indicate that the SiMO and MWCNT molecules cover over the PANI polymer chains. As the result, the morphology of PANI/SiMo/MWCNT can be recognized as a much compact structure.

3.3. Electrocatalytic properties of PANI/SiMO/MWCNT film modified electrode

The electrocatalytic reaction of NADH and H_2O_2 using the PANI/SiMO/MWCNT hybrid film was investigated and compared with PANI, PANI/SiMO, and PANI/MWCNT.

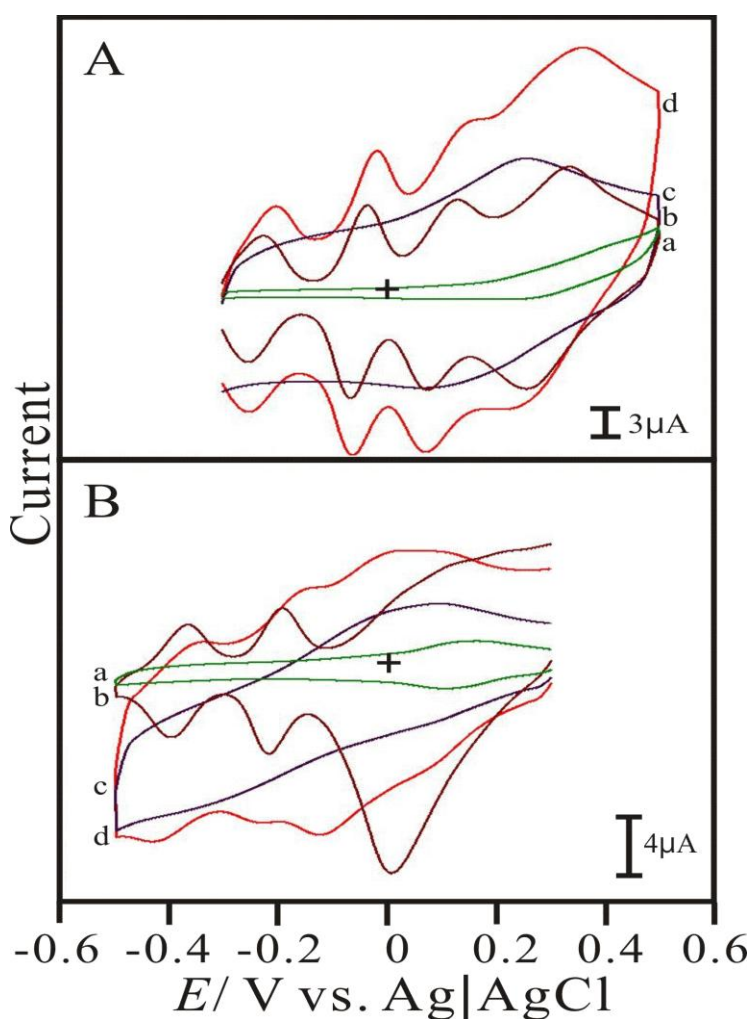


Figure 3. Cyclic voltammograms of (A) 9×10^{-4} M NADH and (B) 6×10^{-3} M H_2O_2 examined in 0.1 M $\text{H}_2\text{SO}_{4(\text{aq})}$ (pH 1.5) with various modified electrodes of (a) PANI/GCE, (b) PANI/SiMO/GCE, (c) PANI/MWCNT/GCE, and (d) PANI/SiMO/MWCNT/GCE, respectively. Scan rate = 0.1 V s^{-1} .

Fig. 3A displays the cyclic voltammograms of NADH electrocatalytic oxidation performed by different modified electrodes in 0.1 M KHP solution (pH 4). The PANI/SiMO/MWCNT shows the higher current response to 9×10^{-4} M NADH. This means that the PANI/SiMO/MWCNT hybrid film is more electroactive than PANI, PANI/SiMO, and PANI/MWCNT for NADH oxidation. As compared with the electrocatalytic reduction of H_2O_2 (Fig. 3B), the PANI/SiMO/MWCNT hybrid film also shows competitive current response to 6×10^{-3} M H_2O_2 . One can conclude that the PANI/SiMo/MWCNT is a good electroactive material due to its good electrocatalytic current response to NADH and H_2O_2 .

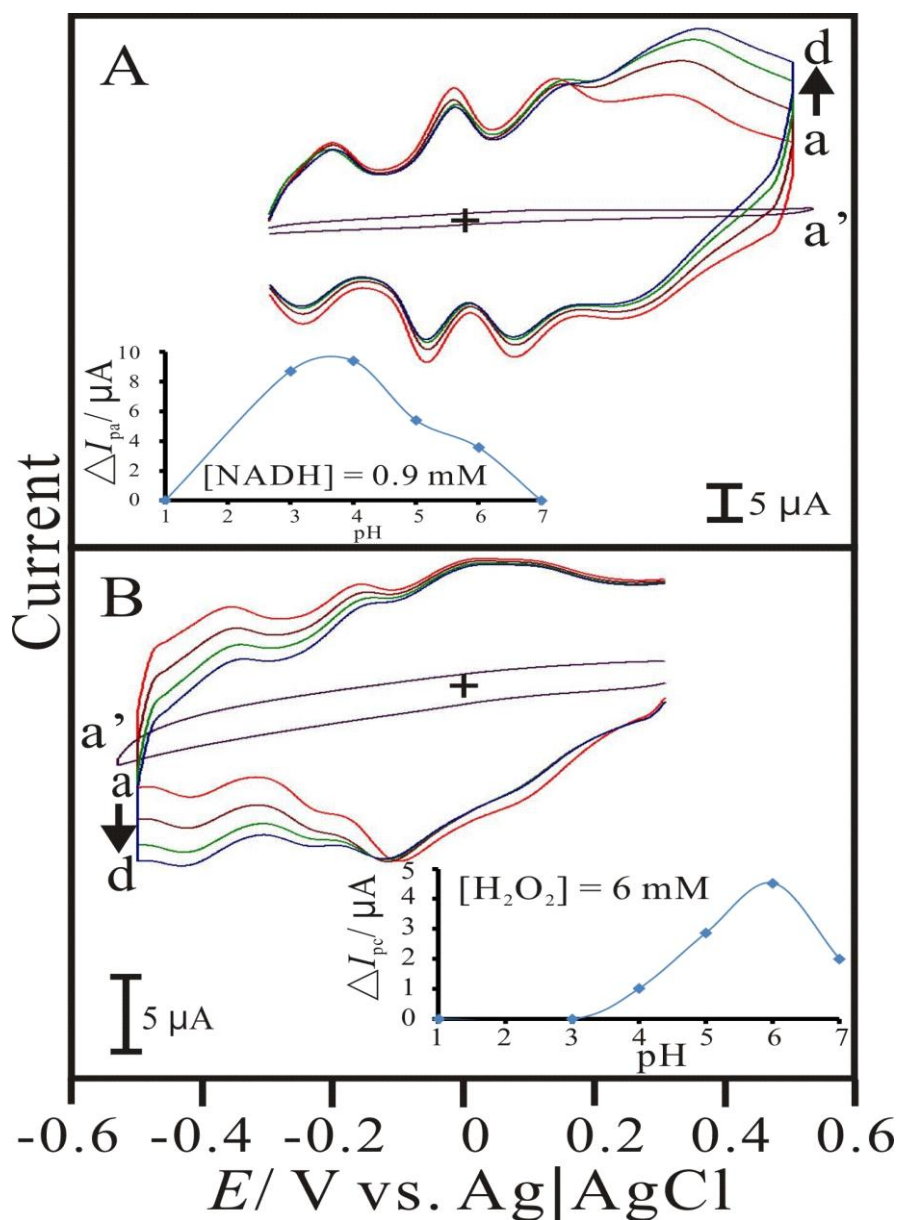


Figure 4. Cyclic voltammograms of PANI/SiMO/MWCNT/GCE examined in 0.1 M $\text{H}_2\text{SO}_4(\text{aq})$ (pH 1.5) containing (A) $[\text{NADH}] =$ (a) 0, (b) 3×10^{-4} M, (c) 6×10^{-4} M, (d) 9×10^{-4} M, and (B) $[\text{H}_2\text{O}_2] =$ (a) 0, (b) 4×10^{-3} M, (c) 8×10^{-3} M, (d) 1.2×10^{-2} M, respectively. Scan rate = 0.1 V s^{-1} . Insets: the plots of the electrocatalytic current change (ΔI_p) vs. pH.

The electrocatalytic property of PANI/SiMO/MWCNT was further studied with different pH conditions. Fig. 4 shows the cyclic voltammograms of PANI/SiMO/MWCNT/GCE examined at pH 4 and pH 6 for NADH and H₂O₂, respectively. It shows one electrocatalytic peak at about +0.35 V for NADH oxidation. As tested in the range of pH 1 – 7 in the presence of 9×10^{-4} M NADH (shown as inset of Fig. 4A), it shows the higher current change (the electrocatalytic current subtracting the blank current) at pH 4. As tested in the presence of 6×10^{-3} M H₂O₂ (shown as inset of Fig. 4B), it shows the higher current change at pH 6. Particularly, it shows two electrocatalytic peaks at about -0.22 V and -0.42 V for H₂O₂ reduction. Compared with bare electrode, this modified electrode shows lower over-potential and higher current response to these species.

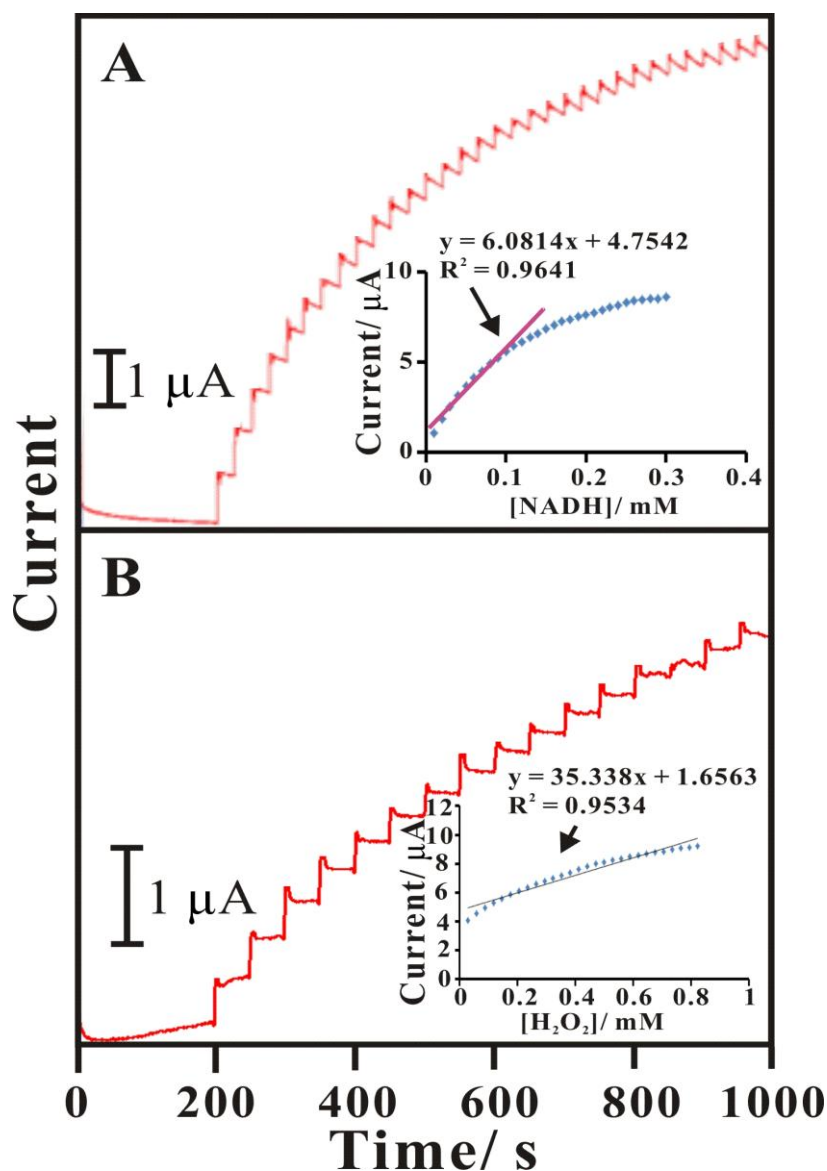


Figure 5. Amperometric response of PANI/SiMO/MWCNT/GCE examined with sequential additions of (A) NADH ($10 \mu\text{M}$ NADH per time, $E_{\text{app.}} = +0.35$ V, pH 4) and (B) H₂O₂ ($29.4 \mu\text{M}$ H₂O₂ per time, $E_{\text{app.}} = -0.35$ V, pH 6), respectively. Electrode rotation rate = 1000 rpm. Time interval = 50 s. Insets: the plots of the electrocatalytic current vs. concentration.

3.4. Amperometric current response of PANI/SiMO/MWCNT/GCE to NADH and H₂O₂

Quantitative determination of NADH and H₂O₂ through PANI/SiMO/MWCNT modified electrode was individually studied by amperometry. Fig. 5A shows the amperograms of PANI/SiMO/MWCNT/GCE examined in 0.1 M KHP (pH 4) with sequential additions of NADH (10 μ M per time, $E_{app.} = +0.35$ V). It was found that the current response was directly proportional to the NADH concentration (inset of Fig. 5A). It shows a linearly concentration range of 0.01 – 0.18 mM with a sensitivity of 222.3 μ A mM⁻¹ cm⁻² and a detection limit of 5 μ M (S/N = 3).

This electrode was also used to determine H₂O₂ by amperometry. Applied potential at -0.35 V, it was found that the current response was directly proportional to the H₂O₂ concentration (inset of Fig. 5B). It also shows a linearly concentration range of 0.0294 – 2.205 mM with a sensitivity of 18.75 μ A mM⁻¹ cm⁻² and a detection limit of 9.2 μ M (S/N = 3). As the result, one can know that the PANI/SiMO/MWCNT hybrid film has potential to develop a bifunctional biosensor for determination of NADH and H₂O₂.

3.5. Stability study of PANI/SiMO/MWCNT film modified electrode

Repetitive redox cycling experiments were done to determine the extent of stability relevant to PANI/SiMO/MWCNT modified GCE in 0.1 M H₂SO₄ solution (pH 1.5). This investigation indicated that after 100 continuous scan cycles with scan rate of 0.1 Vs⁻¹, the peak heights of the cyclic voltammograms decreased less than 8%. On the other hand, the PANI/SiMO/MWCNT modified GCE kept its initiate activity for more than one month as stored in 0.1 M H₂SO₄ solution (pH 1.5). A decrease of 9% was observed in current response of the electrode at the end of 30th day.

4. CONCLUSIONS

Here we report a simple method to prepare the PANI/SiMO/MWCNT hybrid composite. This hybrid film modified electrode is characterized in stable with various scan rates in acidic aqueous solutions. The surface of this hybrid film is rough might be due to the MWCNT aggregation covers over the PANI polymer chains. This film modified electrode shows good electrocatalytic property to NADH and H₂O₂. The optimized pH condition for determining these two species is found different. Particularly, it shows two electrocatalytic peaks to H₂O₂ reduction. This electroactive material has potential to develop a bifunctional biosensor for determination of NADH and H₂O₂.

ACKNOWLEDGEMENTS

This work was supported by the National Science Council of Taiwan (ROC).

1. S. Yao, J. Xu, Y. Wang, X. Chen, Y. Xu, S. Hu, *Anal. Chim. Acta.* 557 (2006) 78.
2. Z. Rosenzweig, R. Kopelman, *Anal. Chem.* 68 (1996) 1408.

3. L. Luo, Z. Zhang, *Anal. Chim. Acta.* 580 (2006) 14.
4. R. Santucci, E. Laurenti, F. Sinibaldi, R.P. Ferrari, *Biochim. Biophys. Acta.* 1596 (2002) 225.
5. J.J. Zhang, Y.G. Liu, L.P. Jiang, J.J. Zhu, *Electrochem. Commun.* 10 (2008) 355.
6. S. Xu, B. Peng, X. Han, *Biosens. Bioelectron.* 22 (2007) 1807.
7. Y.Y. Wang, X.J. Chen, J.J. Zhu, *Electrochem. Commun.* 11 (2009) 323.
8. A. Bergel, J. Souppe, M. Comtat, *Anal. Biochem.* 179 (1989) 382–388.
9. Y. Yan, W. Zheng, L. Su, L. Mao, *Adv. Mater.* 18 (2006) 2639–2643.
10. A. Radoi, D. Compagnone, *Bioelectrochemistry* 76 (2009) 126–134.
11. J. Moiroux, P.J. Elving, *Anal. Chem.* 50 (1978) 1056–1062.
12. Z. Samec, P.J. Elving, *J. Electroanal. Chem.* 144 (1983) 217–234.
13. W.J. Blaedel, R.A. Jenkins, *Anal. Chem.* 47 (1975) 1337–1343.
14. M. Musameh, J. Wang, A. Merkoci, Y. Lin, *Electrochem. Commun.* 4 (2002) 743–746.
15. M.G. Zhang, A. Smith, W. Corski, *Anal. Chem.* 76 (2004) 5045–5050.
16. C. Deng, J. Chen, X. Chen, C. Xiao, Z. Nie, S. Yao, *Electrochem. Commun.* 10 (2008) 907–909.
17. Y.S. Negi, P.V. Adhyapak, *Polym. Rev.* 42 (2002) 35–53
18. S. Bhadra, D. Khastgir, N.K. Singha, J. HeeLee, *Prog. Polym. Sci.* 34 (2009) 783–810
19. N. Oyama, T. Tatsuma, T. Sato, T. Sotomura, *Nature* 373 (1995) 598–600
20. S. Mu, J. Ye, Y. Wang, *J. Power Sources* 45 (1993) 153–159
21. P.K. Rajendra, N. Munichandraiah, *Anal. Chem.* 74 (2002) 5531–5537
22. M. Kanungo, A. Kumar, A.Q. Contractor, *Anal. Chem.* 75 (2003) 5673–5679
23. L. Zhang, X. Jiang, S. Dong, *Biosens. Bioelectron.* 21 (2006) 1107–1115
24. L. Zhang, J.Y. Lian, *J. Electroanal. Chem.* 611 (2007) 51–59
25. L. Zhang, *J Solid State Electrochem.* 11 (2007) 365–371
26. X.J. Feng, Y.L. Shi, Z.A. Hu, *Int. J. Electrochem. Sci.*, 5 (2010) 489–500
27. M. Stočes, K. Kalcher, I. Švancara, K. Vytřas, *Int. J. Electrochem. Sci.*, 6 (2011) 1917–1926
28. X. Wang, Z. Kang, E. Wang, C. Hu, *J. Electroanal. Chem.* 523 (2002) 142–149
29. L. Cheng, J.A. Cox, *Electrochem. Commun.* 3 (2001) 285–289
30. L.M. Abrantes, C.M. Cordas, E. Vieil, *Electrochim. Acta* 47 (2002) 1481–1487
31. S. Dong, L. Cheng, X. Zhang, *Electrochim. Acta* 43 (1998) 563–568
32. M. Barth, M. Lapkowski, S. Lefrant, *Electrochim. Acta* 44 (1999) 2117–2123
33. D. Martel, A. Kuhn, P.J. Kulesza, M.T. Galkowski, M.A. Malik, *Electrochim. Acta* 46 (2001) 4197–4204
34. L. Cheng, S. Dong, *J. Electroanal. Chem.* 481 (2000) 168–176
35. P.J. Kulesza, M. Chojak, K. Miecznikowski, A. Lewera, M.A. Malik, A. Kuhn, *Electrochem. Commun.* 4 (2002) 510–515
36. T.R. Zhang, W. Feng, R. Lu, X.T. Zhang, M. Jin, T.J. Li, Y.Y. Zhao, J.N. Yao, *Thin Solid Films* 402 (2002) 237–241
37. S. Iijima, T. Ichihashi, *Nature* 363 (1993) 603.
38. J.X. Luo, Z.J. Shi, N.Q. Li, Z.N. Gu, Q.K. Zhuang, *Anal. Chem.* 73 (2001) 915.
39. J. Wang, M. Musameh, *Anal. Chem.* 75 (2003) 2075.
40. H.L. Hsu, J.M. Jehng, *Mater. Sci. Eng. C* 29 (2009) 55.
41. Y. Liu, J. Lie, H. Xu, *Talanta* 74 (2007) 965.
42. S. Chen, R. Yuan, Y. Chai, B. Lin, W. Li, L. Min, *Electrochim. Acta* 54 (2009) 3039.
43. F. Xi, L. Liu, Z. Chen, X. Lin, *Talanta* 78 (2009) 1077.
44. Y.T. Chang, K.C. Lin, S.M. Chen, *Electrochim. Acta* 51 (2005) 450–461
45. E. Laviron, *J. Electroanal. Chem.* 52 (1974) 355–393